



## Align a WDS setup and characterise the new capillary at beamline L

Anita Gerényi, Budapest University of Technology and Economics, Hungary

September 6, 2011

### **Abstract**

In the ED detection mode, the energy resolution is around 0.1keV. But in the XRF analysis two fluorescent lines can be so close to each other, that it becomes difficult to calculate the line intensity with the detector energy resolution. That is why in these cases better to use WDS detection mode. This report is about how we set the WDS mode to the Beamline L, and what energy resolution we got in the first setup. Because of a new capillary is used at the beamline, this capillary's transmission and focal spot size also had been determined.

# Contents

|  |    |
|--|----|
| 1. Motivation .....                            | 2  |
| 2. Beamline L at DORIS III .....               | 2  |
| 3. WDS setup.....                              | 3  |
| 3.1 Adjust the WDS setup .....                 | 4  |
| 3.2 The first WDS setup and measurements ..... | 8  |
| 4. New detector capillary parameters .....     | 10 |
| Summary .....                                  | 14 |
| Acknowledgements .....                         | 15 |
| References .....                               | 16 |

## 1. Motivation

In 2011 July and August, as a summer student I joined to the beam research team at Beamline L at the DORIS III storage ring. At the Beamline L, I've got a task to participate in the installation of a new WD-detection set-up. For this work, all the instruments required for this setup were available at the beginning of my activity. My main task was to set and adjust mechanically and optically these technique elements of the detector system at the experimental station of Beamline L and calibrate them in order to perform a real WD measurement. At the meantime a new polycapillary was received, that we installed to the Beamline L setup. For the accurate application of this new X-ray optical element its working parameters had to be determined; this was my next task.

## 2. Beamline L at DORIS III [1]

The Beamline L operates at the DORIS storage ring. It can mainly be used for  $\mu$ XRF and  $\mu$ XANES measurements. The source is from a bending magnet, that able to produce the photon flux density is around  $10^9$  photons/s/mm<sup>2</sup> at the sample.

The synchrotron beam can be monochromatised with crystals (Si 111 or Si 311) or multilayer optics but the white beam can be applied as well. In order to reduce the beam flux, different absorber layers can be applied in the vacuum tank to protect the multilayer against beam-damage. Some cases it is necessary to protect the detector or the sample against the high X-ray flux. For this absorber layer can also be applied after the monochromators. Another possibility to reduce the photon flux is an adjustable slit system that is used to limit the size of the beam to the required size. This type of slit system is mounted before and after the monochromator as well. The minimum size of the beam can be achieved by this slit system is around 20-30  $\mu$ m. To generate a smaller beamsizes in  $\mu$ m range mono- or polycapillary optics is needed. For data evaluation it is important to know the relative variable of the beam intensity (or flux), therefore an ionisation chamber is set before and after the sample to measure continuously the beam signal.

In energy dispersive detection mode Si(Li), HPGe or SDD (Vortex 60/90 ex) is used to measure the fluorescent signal emitted by the irradiated sample. Due to the highest counting capacity of SD detectors in most of the experiments these type of detectors are applied. The energy resolution of SDD is around 140-250 eV and the counting capacity is around few hundredthousand per second without changing the energy calibration. If wavelength dispersive detection is used, there is no need for energy-dispersive detectors and the SDD can be changed to proportional counters. Other, more important advantage of the WDS setup is the much better energy resolution (comparing to the ED detector systems) that is better than the counter's own energy. This advantageous property of WDS allows the deconvolution of the overlapped XRF-lines.

### 3. WDS setup

In these two months we worked on the installation of the basic setup of the wavelength dispersive detection device equipped with SD detector used to the detection of secondary X-ray photons. The main advantage of application of this SD detector is that the full energy-range of the X-ray spectra is detected simultaneously and the scattered signals can be separated. The sketch of the wavelength dispersive device is shown on Figure 1.

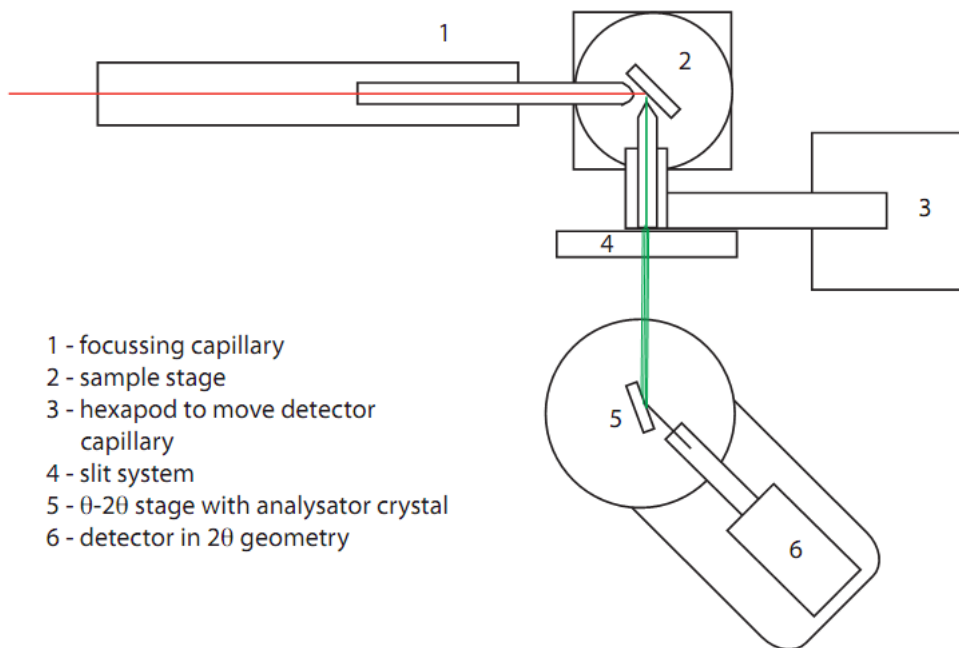


Figure 1. A diagram of the WDS detection system

In confocal measuring geometry the monochromatic synchrotron beam is focused with the first polycapillary (see Fig. 1.) and reaches the sample that is mounted in the focal point of the first capillary. The secondary X-ray radiation emitted by the sample is focused by a 2nd polycapillary that is mounted between the sample and the slit system before the  $\theta$ - $2\theta$  stage unit. This optics unit lies on an arm, which can be moved by a 2<sup>nd</sup> hexapod and the hexapod also can be moved in 3 dimensions by a bigger stage. After this capillary, the beam size has to be reduced with a slit system in order to produce an optimal size of the secondary beam for the WD detection. The dimension of the slit can be set from closed to 6.6mm. After that the beam crosses the crystal (Si111). The main purpose of this slit is to cut the horizontal size of the beam in order to arrange the more precisions the wavelength-selection. After Bragg-reflection on the Si111 crystal, only the selected wavelength reaches the detector. The energy selection is can be implemented with a so called  $\theta$ - $2\theta$  stage.

### 3.1 Adjust the WDS setup

The first step in the construction of the new setup was to connect the motor controllers to the mechanical parts of the moving system. This is a critical point of the assemble procedure due to the fact, that the slit system needs less current than the normal motors, therefore it has to be limited. The motor current was regulated down ( $I_{Drive}$ ) to 0.5 division sign. The motors connections and their moving directions are shown on the Figure 2.

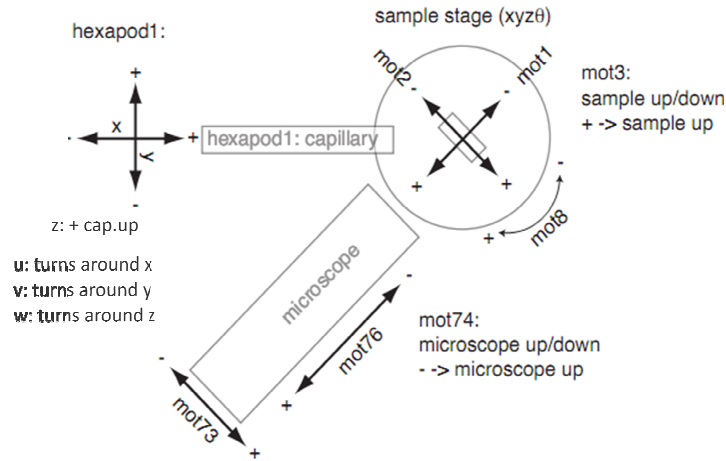


Figure 2.a. The moving direction of hexapod1 with incoming capillary on it, the sample stage and the optical microscope.

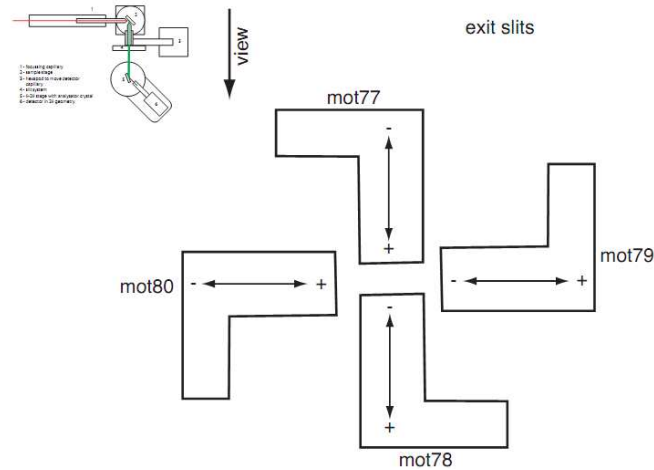


Figure 2.b. Working principle of the slit system with the connected motors for each arm and the direction of their movement.

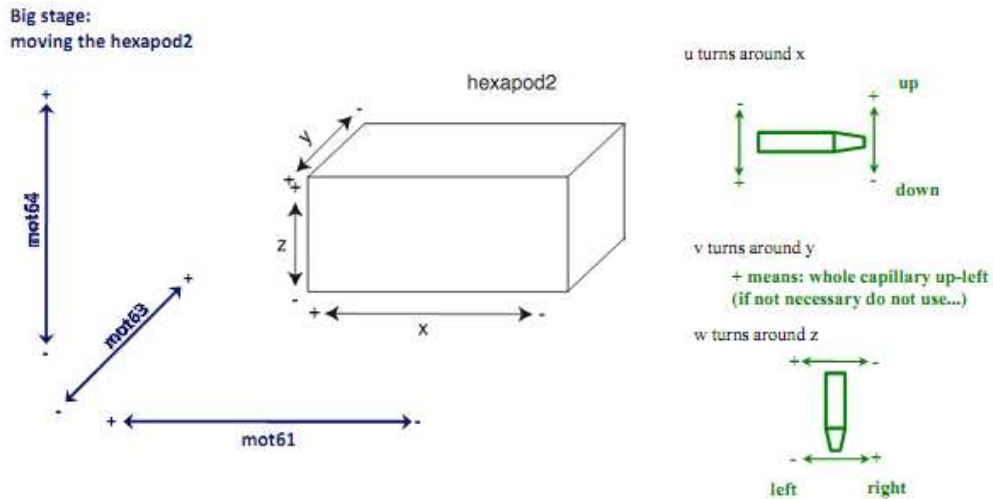


Figure 3.c. Moving the second capillary by the hexapod2 and the big stage, with the connected motors for each arm and the direction of their movement.

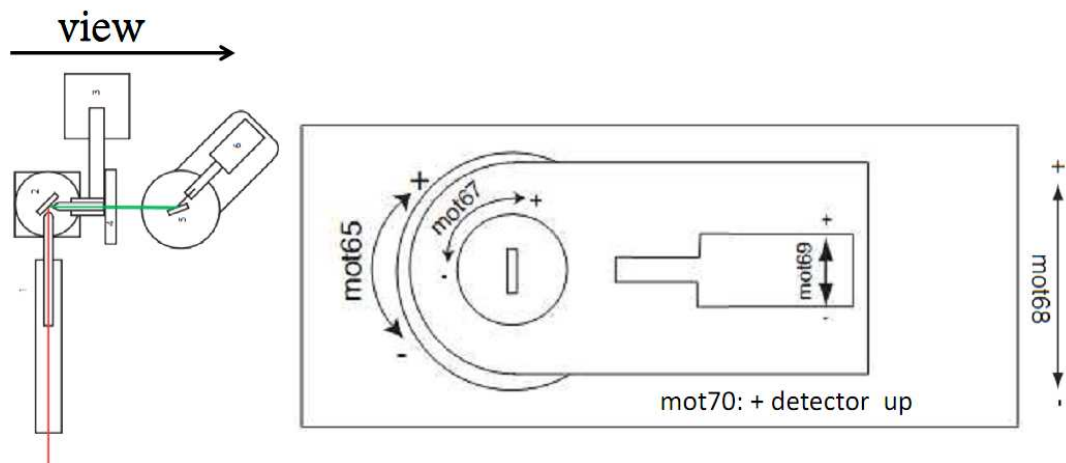


Figure 2.d. 0-20 stage top view, with the crystal and the detector.

In the confocal setup the new detector capillary was used for focusing the incoming beam, and the high-flux capillary was used as the XRF capillary (used for forming the secondary beam before the detector). That was necessary, because the working distance of the detector capillary is around 500 $\mu\text{m}$ , so it extremely difficult task to align it as an XRF capillary with the hexapod2.

The first step was to adjust the position and orientation of the first capillary by the hexapod1. For this reason, the maximum signal level of the second ionisation chamber had to be found by scanning the x, y, v and w direction of the hexapod1 (without sample). One had to be thoughtful not to move out the capillary out of the beam.

After setting the right position of this direction of the capillary, the focal spot distance has to be found with application of a fluorescent screen mounted in the sample position. It has to be

moved to the right optical position that was found by use of the optical microscope. Then by scanning with the hexapod1 x motor, the smallest spot on the fluorescent-screen has to be found.

After the first capillary was set in the right position the XRF capillary has to be adjusted. For this reason, the ED-setup's detector stage was used, because in that case the detector is in closer position to the second capillary than in the WDS setup. Only a simple collimator without pinhole was used; it makes easier to find the beam coming out from the capillary.

The main difficulty in this alignment is that the capillary is on the end of a long arm, therefore it is mechanically sensitive if any mechanical parameter is changed (the hexapod's angle, the angle of the capillary). To avoid this difficulty one should level the capillary-holder with a simple spirit-level. After this action only the  $w$  angle has to align, that should be checked optically that it has to be in the right  $w$  position before starting to move the motors. Then put the capillary to the holder, and try to find the best position by moving hexapod2 x, y, z and  $w$ . The easiest way is to move out from the best focus with  $y$ , set first the  $z$ , after  $w$  and  $x$  and finally the right focus with  $y$ . But one has to be careful with moving out from the focus with  $y$ , because if it is too far, nothing can be seen in the detector sign.

If both capillaries are aligned, the detector unit had to be fit to the WDS stage position. The Si111 wavelength-selection crystal was removed from the stage, then the collimator with the pinhole had to be put in the front of the SD detector. Finally the detector's  $y$  direction was set as parallel with the 2<sup>nd</sup> capillary as possible. The difficulty of this alignment is that the detector's angle can be set only by manually so the parallelism with the second capillary can only be checked optically. Because of the pinhole has to be used in the measurements, it is necessary to align the detector's angle more or less.

In this setup, one has to adjust the detector's position by moving it in its  $x$  (mot 68 and mot69) and  $z$  (mot 70) direction to find the best position.

When the detector is in the right position, the exit slit system can be put into the setup. Only the open/close of the slit can be controlled by motors, so one has to put it in a right  $x$  and  $z$  position manually. The easiest way of this adjustment is to remove the collimator (and the pinhole) from the detector, and open the slit to its limit. If the slit is in right position, the SDD's counting level is almost the same as it was before the slit.

The size of the slit has to be closed to  $\sim 1$ mm size horizontally. The vertical size has no influence to the angle resolution of the setup. The slit's motors movements are  $\sim 0.1$  mm / 0.575 steps. The limits of the movements are shown in the Table 1.

|       | min | max      | distance |
|-------|-----|----------|----------|
| mot77 | 0   | 17.087   | ~3 mm    |
| mot78 | 0   | -14.0315 | ~2.5 mm  |
| mot79 | 0   | -29.0485 | ~5 mm    |
| mot80 | 0   | 20.06    | ~3.5 mm  |

Table 1. The movement limits of the slit's motors

If the adjustment of the slit is completed, the detector has to be aligned again.

Next step is to place the crystal. There is a sign on the goniometer stage where should it be. In this case to find the right position of the crystal is a bit more complicated. The crystal has to be moved in x direction between the slit and the detector. Because of the whole  $\theta$ - $2\theta$  stage is in one x-direction moving stage (mot69), the detector and the crystal can only together move. The detector also has its own x-direction movement motor (mot68) on the stage, therefore when the whole stage is moved; the detector can be moved back to its original position. In this case only the crystal is moving. For this automatic scan, combined scan has to be done using mot 68 and mot69, with the factor +1. Before using this scan, one has to check that these two motors have the same step size. If these two values are not equal, the ratio between the motor counts and the movement has to be changed.

During this combined scan the crystal moved to direction of the beam (the first peak of the derivated of the scan-sign). Then one has to check the crystal's angle. For this purpose, the signal of the detector has to be measured while the crystal's angle is being changed. The scan result can be seen on figure 3. The right angle is the maximum of the curve. After the angle alignment the position of the crystal should be align again to the maximum of the derivate curve.

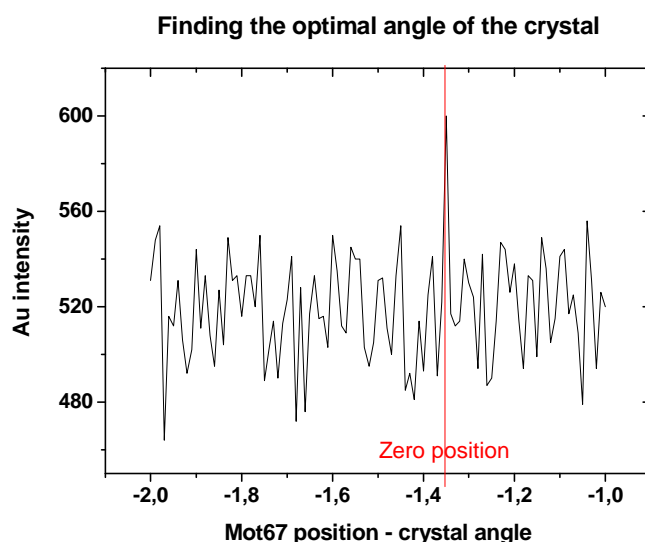


Figure 3. The search of the right crystal angle position. The maximum of the curve indicate the required parallel position.



The final step of the adjustment procedure is to calibrate the  $\theta$ - $2\theta$  angles to wavelength/energy units. Set the required angle with mot67 and change mot65. Again combined scan has to be used with mot65 and mot67 for moving the  $\theta$  and  $2\theta$  angle. In this case, to let the  $\theta$ - $2\theta$  change together, the factor between mot65 and mot67 should be +0.5. To the first, low resolution scan with 0.05 step size can be used on mot65 as  $2\theta$ . If the selected angle has found, a lower step-size scan should be done to determine the angle resolution.

After this complex setup, the WDS based measurements can be started. Combined scan has to be used with mot67 and mot65. The lowest motor step size is 0.0005, all of the two motors, so the lowest step-size scan is 0.001 on motor67 and 0.0005 on motor65. The combined scans factor is +0.5.

### 3.2 The first WDS setup and measurements

For the first test measurement we used thick gold foil to adjust the setup and determine the right motor positions. The energy of the applied primary synchrotron beam was set to 15 keV. The energies of gold L lines, wavelengths and the calculated theta and  $2\theta$  angles are shown on the Table 2.

|               | Au L $\alpha$ 1 | Au L $\alpha$ 2 | Au L $\beta$ 1 | Au L $\beta$ 2 |
|---------------|-----------------|-----------------|----------------|----------------|
| E [keV]       | 9,7133          | 9,628           | 11,442         | 11,585         |
| $\theta$ °    | 11,744          | 11,850          | 9,950          | 9,826          |
| $2\theta$ °   | 23,489          | 23,700          | 19,900         | 19,653         |
| Intensity (%) | 100             | 11              | 67             | 23             |

Table 2 – Energies of the gold L lines, relative intensities, value of the total reflection's angle from Si-111 crystal ( $\theta$ ) and the detection angle ( $2\theta$ ).

The relation between the energies and the wavelengths given by equation (1)

$$\theta [^\circ] = \frac{180^\circ}{4\pi} \arcsin \left( c \cdot h \cdot \frac{1}{E[\text{keV}]/1000/2d} \right) \quad (1)$$

where  $c=299792458\text{m/s}$   $h=4.14 \cdot 10^{-15}\text{eVs}$   $2d=6.271 \cdot 10^{-10}\text{m}$

First, we found the Au-L $\beta$ 1 and L $\beta$ 2 wavelength and checked the shift between the angle calculated from the motor position and the real angle. The  $2\theta$  angle calculated from the energy should be  $19.9^\circ$  to the more intensive L $\beta$ 1 line, but from the measurement, the motor position is different ( $21.861^\circ$ ). So we calibrate the motors (67 and 65) position to the right angles. After this, the positions of the motors give the right  $\theta$  and  $2\theta$  angles.

To get more energy points, we also measured Fe samples K-edge energies. The energy-angle relation is shown in Table 3.

|               | Fe K $\alpha$ 2 | Fe K $\alpha$ 1 | Fe K $\beta$ 1 |
|---------------|-----------------|-----------------|----------------|
| E [keV]       | 6,391           | 6,40384         | 7,05798        |
| $\theta$ °    | 18,021          | 17,983          | 16,268         |
| 2 $\theta$ °  | 36,042          | 35,966          | 32,535         |
| Intensity (%) | 50              | 100             | 17             |

Table 3 – Iron K lines energies, their relative intensities, value of the total reflection's angle from Si-111 crystal ( $\theta$ ) and the detection angle (2 $\theta$ ).

To determine the energy resolution of this new setup, the curves has to be fit with double-voigt functions, and the FWHM of these functions add the energy dependent energy resolution. The fitting of the four lines can be seen at Figure 4.

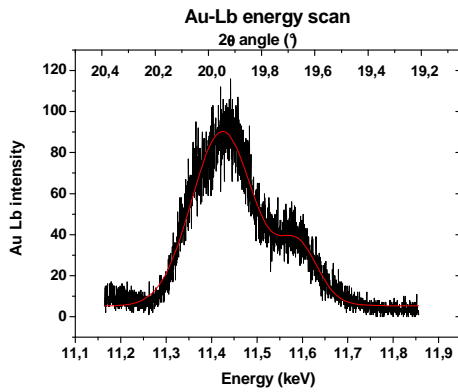


Figure 4.a. The measured intensity of the Au L $\beta$  lines by changing the selected wavelength.

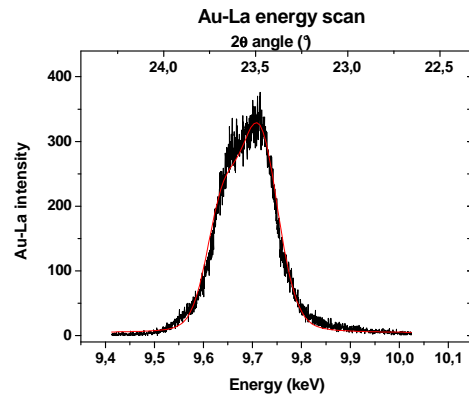


Figure 4.b. The measured intensity of the Au L $\alpha$  lines by changing the selected wavelength.

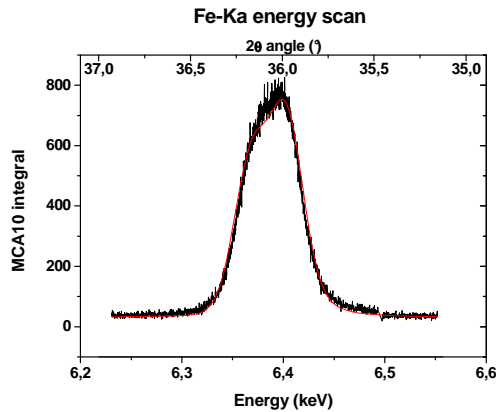


Figure 4.c. The measured intensity of the Fe K $\alpha$  lines by changing the selected wavelength.

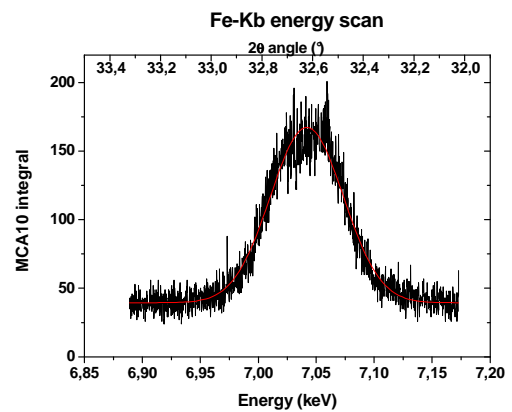


Figure 4.d. The measured intensity of the Fe K $\beta$  lines by changing the selected wavelength.

Figure 5 shows the energy resolution as a function of the line energy/wavelength.

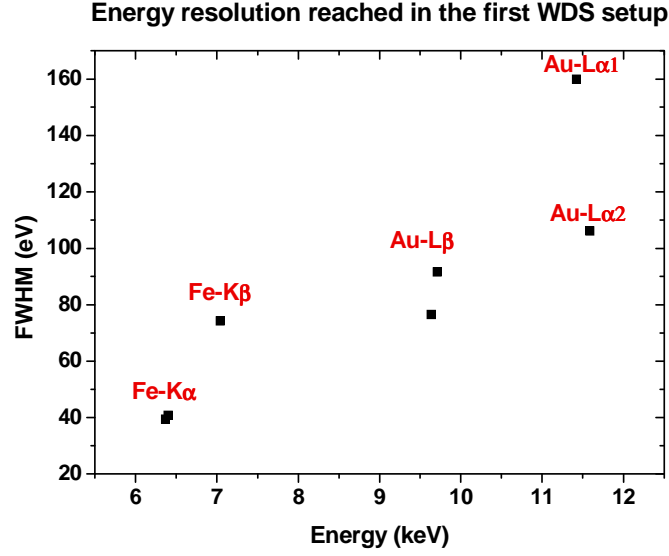


Figure 5. The Energy resolution of the WDS setup

The lines are very close to each other, and in the same time the statistic of the points are not sufficient, therefore the fitting result is very sensitive to the line energy value. To achieve more accurate wavelength-resolution results, longer measuring time should be used in the measurements. However the energy resolution we got, is consistent with other WDS setup with one Si111 crystal at the beamline ID21 (ESRF) [2].

One possible way of increasing the count rate is to change the two capillaries. Using the high flux capillary as a first capillary, means higher beam intensity at the sample, than using the detector capillary as an incoming capillary.

#### 4. New detector capillary parameters

Because a new capillary was applied in this new system, its parameters had to be measured. This polycapillary should be used later as an XRF capillary, so the applied energy range is around the most commonly used XRF lines-energies. We tested the transmission property and the focal spot size at 10keV and 17keV.

In order to determine the transmission feature of the capillary, we measured the level of C2 and C4 ionisation chambers signal with the capillary and without it. Without the capillary the relation between the C2 and C4 signs shows the absorption between the two ionisation chambers. By using the capillary, the change in the signals ratio gives the effect of the capillary's transmission. The transmission at 17keV is 39.33% and at 10keV is 18.75%. It is higher than it can be expected from the manual's ~8% at 8keV. To make sure in get the right value, it should be measured and calculated again later.

To determine the focal spot size, edges of different samples were measured [3]. For this purpose at energy of 10 keV we used a 4  $\mu\text{m}$  wolfram wire, pure Au-cross sample and a thin Co sample. At energy of 17 keV we determined this parameter only with the Au-cross and the W-wire. On the basis of the measurements, the W-wire seems to be more correct. First time the y, z, u, v, w positions of the capillary were set, and after the x position. The samples edges were changed with scanning by mot2 or mot3. This purpose the sign of both of the C4 counter or the SDD detector can be used.

The results of measurement of the W-wire showed a Gaussian curve therefore I fit this type of function to the values of the signal. The FWHM of this curve was accepted as the size of the focal spot. The measured and fit curves are shown on Figure 6.

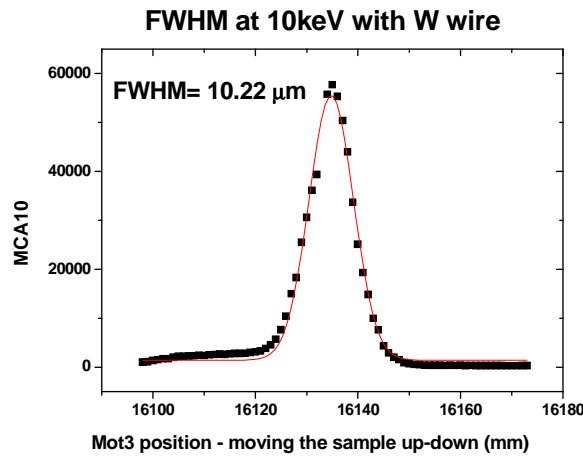


Figure 6.a At 10 keV the measured FWHM with W wire

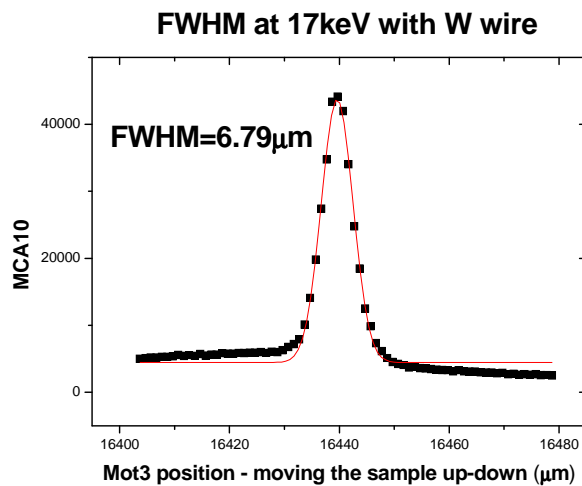


Figure 6.b At 17 keV the measured FWHM with W wire

In case of the Au sample, the sample was moving along the beam direction. The fluorescence signal was measured, therefore the curve has to be derivated, and the Gaussian curve should fit to this derivated-curve (see Fig. 7).

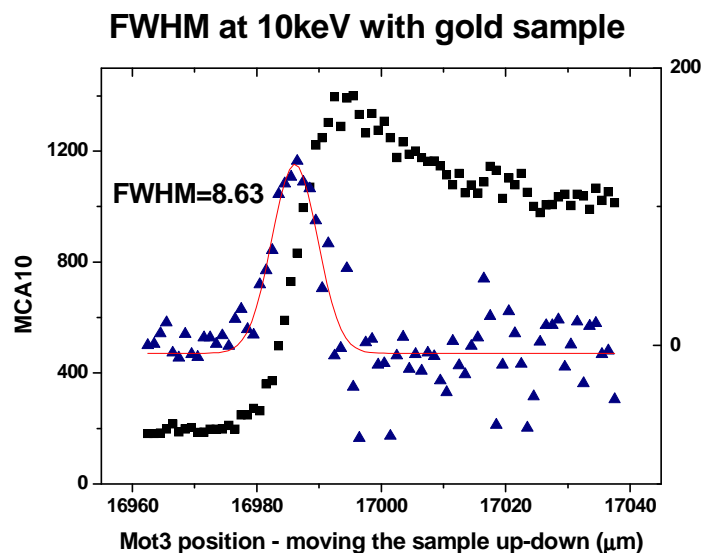


Figure 7.a. At 10 keV the measured FWHM with Au sample

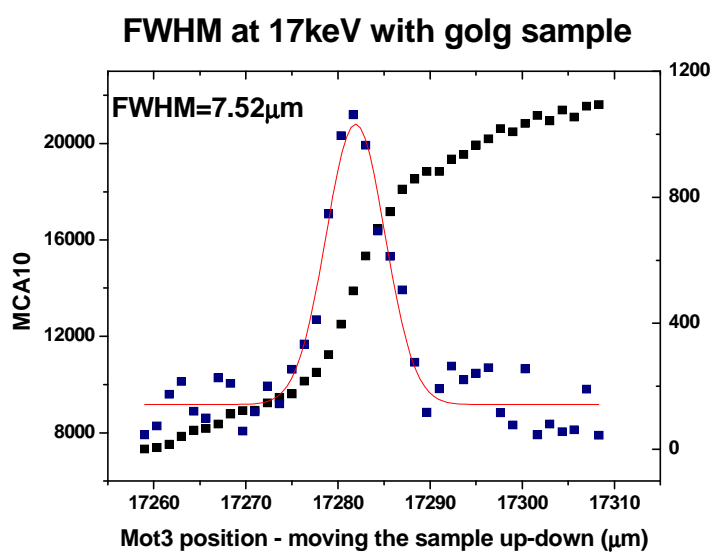


Figure 7.b. At 17 keV the measured FWHM with Au sample

The change of the focal spot size by changing the capillary's distance from the sample is shown at Figure 8 at the 2 energies in the case of the W wire.

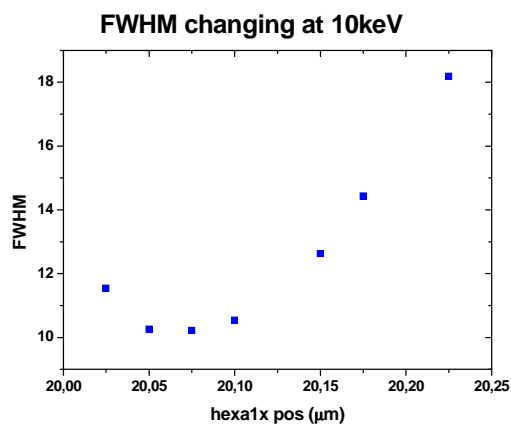


Figure 8.a. The focal spot size by changing the capillary-sample distance at 10 keV

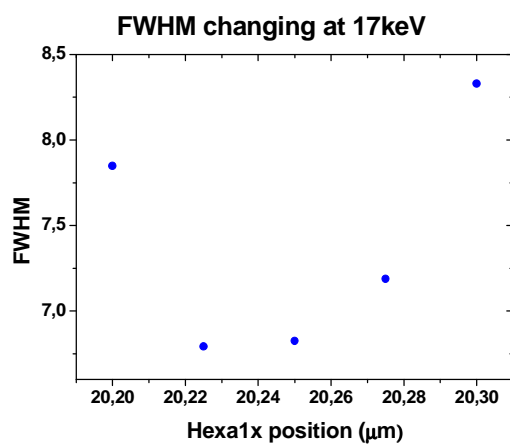


Figure 8.b. The focal spot size by changing the capillary-sample distance at 17 keV

## **Summary**

The first alignment of the WDS setup was successful, but in order to achieve more correct operation parameters the setup should be aligned more precisely than we did at the first time. To increase the level of detector signals the high flux capillary has to be used as an incoming capillary for forming the synchrotron beam, and the new detector capillary must be used as an XRF capillary for forming the secondary X-ray beam (emitted by the sample). In this case the signal level of the detector should be higher; therefore the determination of the energy-resolution of the detector system should be more precisely.

## **Acknowledgements**

I spent a very nice time at DESY at Beamline L. I would like to thank my supervisors, Karen Appel and Manuela Borchert, that they introduced me so many technical details and methods of setting up the setup of beamline L. I am glad that I could join to this project aiming the calibration of this new WDS detection system at the beamline. I hope, I will be able to utilize this new knowledge in the next future when we will perform our research project at the beamline.

And finally thanks all of the summerstudents to make our time very nice.



## References

- 
- [1] [http://hasylab.desy.de/facilities/doris\\_iii/beamlines/l\\_hymo/index\\_eng.html](http://hasylab.desy.de/facilities/doris_iii/beamlines/l_hymo/index_eng.html)
  - [2] J. Szlachetko et al., Wavelength-dispersive spectrometer for X-ray microfluorescence analysis at the X-ray microscopy beamline ID21 (ESRF), *Journal of Synchrotron radiation*, 2010
  - [3] G. Falkenberg, More polycapillary half-lenses for the hard X-ray microprobe at beamline L